

INORGANIC SYNTHESIS
AND INDUSTRIAL INORGANIC CHEMISTRY

Thermochemical Behavior of Crystalline Copper–Zinc Complexes of Nitrilotris(methylenephosphonic) Acid

F. F. Chausov^{a,*}, I. S. Kazantseva^a, N. V. Lomova^a,
A. V. Kholzakov^a, I. N. Shabanova^a, and N. E. Suksin^a

^a Udmurt Federal Research Center, Ural Branch, Russian Academy of Sciences,
Izhevsk, Udmurt Republic, 426068 Russia
*e-mail: chaus@udman.ru

Received February 9, 2022; revised May 26, 2022; accepted June 5, 2022

Abstract—The thermal behavior and mechanism of decomposition of crystalline heterometallic chelate complexes in the concentration substitution series $\text{Na}_4[\text{Cu}_x\text{Zn}_{1-x}\text{N}(\text{CH}_2\text{PO}_3)_3] \cdot 13\text{H}_2\text{O}$ ($0 < x < 1$) were studied by thermal gravimetric and differential thermal analysis and by X-ray photoelectron spectroscopy. The decomposition temperature depends on the composition of the heterometallic complexes and configuration of dimeric clusters in their crystal lattice. The heterometallic complex with $x = 1/4$ shows the highest thermal stability (decomposition onset at approximately 280°C) because of the lowest strain in the structure of the complex anion. Changes in the chemical composition of the complex with $x = 1/2$, whose crystal structure is built of clusters of identical composition, starts already at 250–290°C, but gaseous products are released only at 300–408°C.

Keywords: nitrilotris(methylenephosphonic) acid, copper–zinc complexes, thermal decomposition, X-ray photoelectron spectroscopy

DOI: 10.1134/S1070427222040073

Zinc complexes with nitrilotris(methylenephosphonic) acid $\text{N}(\text{CH}_2\text{PO}_3)_3\text{H}_6$ (NTP) are effective corrosion inhibitors in neutral aqueous media [1, 2] and are widely used in that capacity in industry. Zinc nitrilotris(methylenephosphonic) acid complexes of different structure differ in the anticorrosion activity under equal other conditions. The most effective corrosion inhibitor is the complex $\text{Na}_4[\text{ZnN}(\text{CH}_2\text{PO}_3)_3] \cdot 13\text{H}_2\text{O}$ with the chelate structure of the inner coordination sphere [3]. Copper nitrilotris(methylenephosphonic) acid complexes, including the chelate complex $\text{Na}_8[\text{CuN}(\text{CH}_2\text{PO}_3)_3]_2 \cdot 19\text{H}_2\text{O}$ [4], are known as bactericides acting, in particular, against sulfate-reducing bacteria.

Because Cu(II) and Zn(II) can form in many cases complexes of similar structure, it is interesting to prepare heterometallic complexes $\text{Na}_4[(\text{Cu},\text{Zn})\text{N}(\text{CH}_2\text{PO}_3)_3]$ and study complexes in the concentration substitution series $\text{Na}_4[\text{Cu}_x\text{Zn}_{1-x}\text{N}(\text{CH}_2\text{PO}_3)_3]$ ($0 < x < 1$). It has been shown that heterometallic copper–zinc complexes form a

fully isomorphous series of mixed crystals $\text{Na}_4[\text{Cu}_x\text{Zn}_{1-x}\text{N}(\text{CH}_2\text{PO}_3)_3] \cdot 13\text{H}_2\text{O}$ ($0 < x < 1$), including isomorphous end members $\text{Na}_4[\text{ZnN}(\text{CH}_2\text{PO}_3)_3] \cdot 13\text{H}_2\text{O}$ and $\text{Na}_4[\text{CuN}(\text{CH}_2\text{PO}_3)_3] \cdot 13\text{H}_2\text{O}$ [5]. The copper content of the crystalline product is virtually proportional to the copper concentration in the solution, suggesting no significant energy barriers to mutual substitution of metal atoms in the crystal [5]. This fact opens prospects for the commercial preparation of uniform batches of crystalline copper–zinc nitrilotris(methylenephosphonic) acid complexes with the preset Cu : Zn ratio and structure ensuring the best anticorrosion properties.

Favorable combination of anticorrosion and bactericidal properties can be expected for such crystalline compounds, which can give significant economic benefit when using them in heat engineering and water recycling systems, cooling systems with cooling towers, and systems for collecting stratal water and maintaining stratal pressure at oil and gas fields. The

use of coordination compounds as corrosion inhibitors in such systems is associated with different temperature conditions of storage and dosage. Hence, to reach the maximum possible performance of these inhibitors, it is necessary to know the features of their thermal behavior, including the decomposition onset temperature and the mechanism and products of thermal decomposition of complexes of different composition.

The decomposition temperature of monometallic copper and zinc nitrilotris(methylenephosphonic) acid complexes depends on the geometric structure of the coordination polyhedron of the metal atom [6]. Monometallic copper and zinc chelates with fully deprotonated nitrilotris(methylenephosphonic) acid are dimeric in the crystal. The coordination polyhedron of the metal atom is a distorted trigonal bipyramid with the metal atom in the center, three oxygen atoms of different PO_3 groups of the nitrilotris(methylenephosphonic) acid molecule in the basal positions, the nitrogen atom of the same ligand molecule in one of the apical positions, and the oxygen atom of one of PO_3 groups of the adjacent nitrilotris(methylenephosphonic) acid molecule in the dimer in the other apical position [2]. The distortion pattern of the trigonal bipyramid in the zinc and

copper complexes is different: In the zinc complex, the coordination polyhedron is elongated along the Zn–N bond [2], and in the copper complex, along one of the Cu–O bonds in the base of the trigonal bipyramid [4].

Because the thermal stability and thermal decomposition mechanism of nitrilotris(methylenephosphonic) acid complexes depend on the structure of the coordination polyhedron, the thermochemical behavior of heterometallic complexes $\text{Na}_4[\text{Cu}_x\text{Zn}_{1-x}\text{N}(\text{CH}_2\text{PO}_3)_3] \cdot 13\text{H}_2\text{O}$ will apparently differ from that of the end members of the isostructural series, $\text{Na}_4[\text{ZnN}(\text{CH}_2\text{PO}_3)_3] \cdot 13\text{H}_2\text{O}$ and $\text{Na}_4[\text{CuN}(\text{CH}_2\text{PO}_3)_3] \cdot 13\text{H}_2\text{O}$. In the isomorphous substitution series $\text{Na}_4[\text{Cu}_x\text{Zn}_{1-x}\text{N}(\text{CH}_2\text{PO}_3)_3] \cdot 13\text{H}_2\text{O}$, the distortion pattern varies gradually as x is increased from 0 to 1. As a result, the distortions compensate each other to certain extent, and the coordination polyhedron becomes the closest to the regular trigonal bipyramid at a certain intermediate value of x [5] (Fig. 1). An interesting structural feature of heterometallic complexes $\text{Na}_4[\text{Cu}_x\text{Zn}_{1-x}\text{N}(\text{CH}_2\text{PO}_3)_3] \cdot 13\text{H}_2\text{O}$ is that the oxygen atoms O^7 , O^8 , and O^9 of one of the phosphonate groups in the ligand molecule are disordered over sites A and B, whereas in the position of the oxygen atoms of the other two phosphonate groups there is no disordering. In the structure of the monometallic zinc and copper complexes, none of the phosphonate groups are disordered. The main distances in the coordination surrounding of the metal atom are given in Table 1.

This study deals with the thermochemical behavior of heterometallic complexes in the concentration substitution series $\text{Na}_4[\text{Cu}_x\text{Zn}_{1-x}\text{N}(\text{CH}_2\text{PO}_3)_3] \cdot 13\text{H}_2\text{O}$.

EXPERIMENTAL

Nitrilotris(methylenephosphonic) acid (pure grade, Wuhan Mulei New Material Co., China) was recrystallized twice before use to reduce the PO_4^{3-} content below 0.3%. ZnO (analytically pure grade, Vekton, Russia), $\text{Cu}_2\text{CO}_3(\text{OH})_2$ (analytically pure grade, Vekton), NaOH (chemically pure grade, Bashkir Soda Company, Russia), dimethyl sulfoxide (chemically pure grade, Kupavnaaktiv, Russia), ethylenediaminetetraacetic acid disodium salt (Na_2EDTA , chemically pure grade, Reakhim, Russia), 4-(2-pyridylazo)resorcinol (PAR) indicator (analytically pure grade, Tatkhimprodukt, Russia), Eriochrome Black T indicator (analytically pure grade, Tatkhimprodukt), $\text{Na}_2\text{S}_2\text{O}_4$ (EKOS-Ural, Russia),

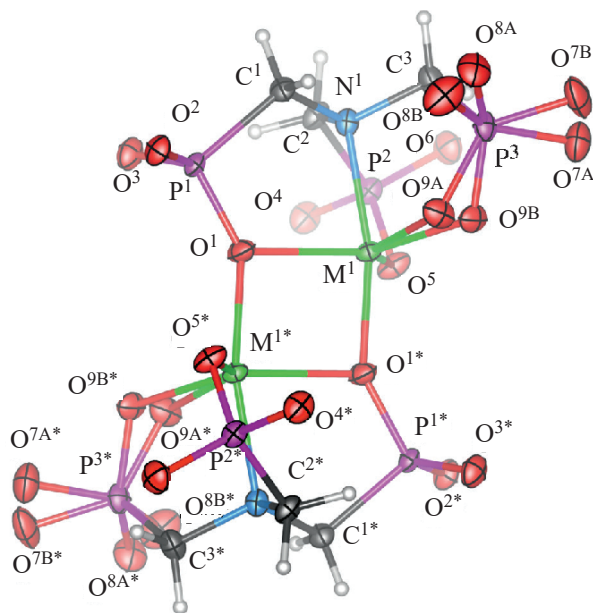


Fig. 1. Dimeric structure of the complex anion $[\text{Cu}_x\text{Zn}_{1-x}\text{N}(\text{CH}_2\text{PO}_3)_3]_2^{8-}$ in the structure of heterometallic zinc and copper complexes with nitrilotris(methylenephosphonic) acid, according to data of single crystal X-ray diffraction analysis [5]. The atoms occupying the symmetrically equivalent position $-x, -y, -z$ are marked with an asterisk.

Table 1. Selected interatomic distances d , Å, in compounds of the series $\text{Na}_4[\text{Cu}_x\text{Zn}_{1-x}\text{N}(\text{CH}_2\text{PO}_3)_3] \cdot 13\text{H}_2\text{O}$ at $x = 0-1$, according to data of single crystal X-ray diffraction analysis [5]

Position (Fig. 1)	x				
	0	¼	½	¾	1
$d(\text{M}^1-\text{N}^1)$	2.2549(8)	2.1132(10)	2.0921(9)	2.0410(15)	2.0111(10)
$d(\text{M}^1-\text{O}^{9A})$	2.0181(8)	1.9869(16)	1.9950(14)	2.0063(17)	2.0088(8)
$d(\text{M}^1-\text{O}^{1*})$	2.0150(7)	1.9793(8)	1.9681(8)	1.9427(13)	1.9263(8)
$d(\text{M}^1-\text{O}^1)$	2.0882(5)	2.1151(9)	2.1336(9)	2.1655(13)	2.1933(8)
$d(\text{M}^1-\text{O}^5)$	1.9880(8)	1.9811(11)	1.9821(10)	1.9738(17)	1.9730(8)

Table 2. Results of elemental analysis of crystalline compounds $\text{Na}_4[\text{ZnN}(\text{CH}_2\text{PO}_3)_3] \cdot 13\text{H}_2\text{O}$ (ZnNTP), $\text{Na}_4[\text{Cu}_x\text{Zn}_{1-x}\text{N}(\text{CH}_2\text{PO}_3)_3] \cdot 13\text{H}_2\text{O}$ ($\text{Cu}_x\text{Zn}_{1-x}\text{NTP}$), and $\text{Na}_4[\text{CuN}(\text{CH}_2\text{PO}_3)_3] \cdot 13\text{H}_2\text{O}$ (CuNTP)

Compound	ZnNTP	$\text{Cu}_x\text{Zn}_{1-x}\text{NTP}$							CuNTP
Mole fraction [Cu]/([Cu] + [Zn]) in reaction mixture	0	0.125	0.25	0.375	0.5	0.625	0.75	0.875	1
Found, wt %									
P	13.6 ± 0.5	13.6 ± 0.5	13.7 ± 0.5	13.6 ± 0.5	13.6 ± 0.5	13.7 ± 0.5	13.6 ± 0.5	13.6 ± 0.5	13.5 ± 0.5
Zn	9.7 ± 0.2	8.6 ± 0.2	7.1 ± 0.2	6.2 ± 0.2	4.6 ± 0.2	4.0 ± 0.2	2.6 ± 0.2	1.4 ± 0.2	0.0 ± 0.2
Cu		0.9 ± 0.2	2.4 ± 0.2	3.3 ± 0.2	4.8 ± 0.2	5.4 ± 0.2	6.7 ± 0.2	7.9 ± 0.2	9.7 ± 0.2
Mole fraction [Cu]/([Cu] + [Zn]) in crystalline product	0	0.100	0.253	0.350	0.515	0.585	0.725	0.852	1
Calculated for $\text{Na}_4[\text{Cu}_x\text{Zn}_{1-x}\text{N}(\text{CH}_2\text{PO}_3)_3] \cdot 13\text{H}_2\text{O}$ at given x									
P	13.57	13.58	13.58	13.59	13.59	13.60	13.60	13.61	13.61
Zn	9.55	8.60	7.14	6.21	4.64	3.97	2.63	1.42	–
Cu	–	0.92	2.35	3.25	4.79	5.44	6.74	7.93	9.31

and gaseous argon (supreme grade, Technical Gases, Russia) were used without additional purification.

The complex $\text{Na}_4[\text{ZnN}(\text{CH}_2\text{PO}_3)_3] \cdot 13\text{H}_2\text{O}$ was synthesized as described previously [2].

The complex $\text{Na}_4[\text{CuN}(\text{CH}_2\text{PO}_3)_3] \cdot 13\text{H}_2\text{O}$ was prepared by the reaction of $\text{Cu}_2\text{CO}_3(\text{OH})_2$ with nitrilotris(methylenephosphonic) acid and NaOH according to [5].

$\text{Na}_4[\text{Cu}_x\text{Zn}_{1-x}\text{N}(\text{CH}_2\text{PO}_3)_3] \cdot 13\text{H}_2\text{O}$ heterometallic complexes were prepared by dissolving weighed portions of the complexes $\text{Na}_4[\text{ZnN}(\text{CH}_2\text{PO}_3)_3] \cdot 13\text{H}_2\text{O}$ and $\text{Na}_4[\text{CuN}(\text{CH}_2\text{PO}_3)_3] \cdot 13\text{H}_2\text{O}$, taken in the ratio

corresponding to the chosen value of x , in a small amount of water. The resulting solution was allowed to stand for 24 h, equal volume of dimethyl sulfoxide was added, and crystals of the mixed complex were grown by slow evaporation of the solvent at room temperature. Heterometallic complexes $\text{Na}_4[\text{Cu}_x\text{Zn}_{1-x}\text{N}(\text{CH}_2\text{PO}_3)_3] \cdot 13\text{H}_2\text{O}$ are transparent triclinic crystals of the color from light yellowish-green (at low values of x) to bright green (at x close to unity).

Elemental analysis of the products was performed by the complexometric method similar to that described previously for quantitative determination of copper and nickel in heterometallic complexes with nitrilotris(meth

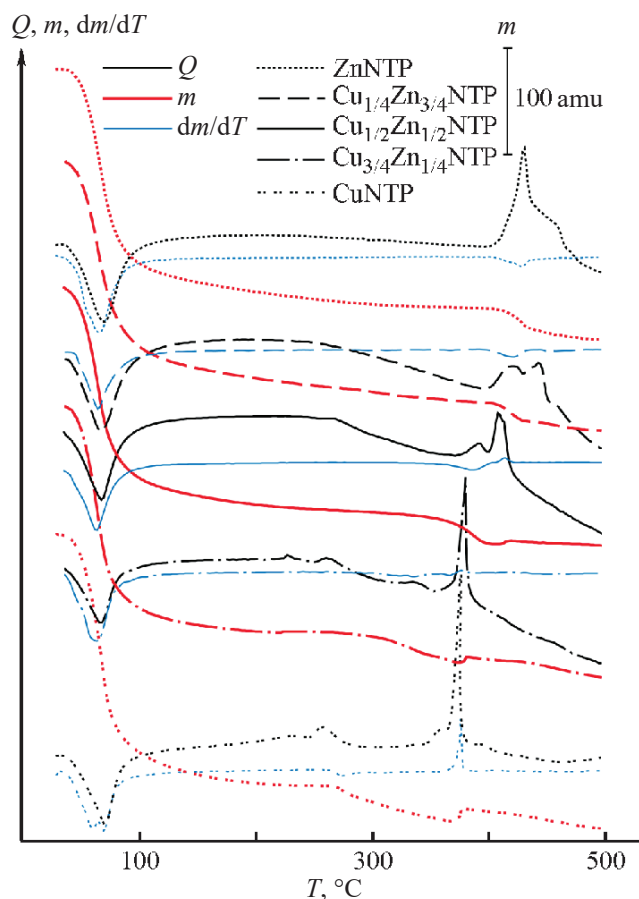


Fig. 2. Thermograms of the heterometallic complexes $\text{Na}_4[\text{Cu}_x\text{Zn}_{1-x}\text{N}(\text{CH}_2\text{PO}_3)_3] \cdot 13\text{H}_2\text{O}$ ($\text{Cu}_x\text{Zn}_{1-x}\text{NTP}$) at $x = 1/4, 1/2,$ and $3/4$ in comparison with those of the complexes $\text{Na}_4[\text{ZnN}(\text{CH}_2\text{PO}_3)_3] \cdot 13\text{H}_2\text{O}$ (ZnNTP) and $\text{Na}_4[\text{CuN}(\text{CH}_2\text{PO}_3)_3] \cdot 13\text{H}_2\text{O}$ (CuNTP) [6].

ylenephosphonic) acid [7]. The crystalline samples were broken down by boiling with an acidified $(\text{NH}_4)_2\text{S}_2\text{O}_8$ solution. The $\text{Cu}^{2+} + \text{Zn}^{2+}$ sum was determined by titration with Na_2EDTA at pH 5.0–6.0 in the presence of 4-(2-pyridylazo)resorcinol indicator. The Zn^{2+} content was determined after complete precipitation of copper with excess $\text{Na}_2\text{S}_2\text{O}_4$ [8, 9] by titration with Na_2EDTA at pH 8.0–9.0 in the presence of Eriochrome Black T indicator. The Cu^{2+} content was determined by calculation. The elemental analysis results are given in Table 2.

The results of single crystal X-ray diffraction analysis have been filed at the Cambridge Crystallographic Data Centre (CCDC) [10]. VESTA 3.5.7 program was used for imaging of molecular structures determined by X-ray diffraction analysis.

Thermal gravimetric and differential thermal analysis of the crystalline products was performed on

a Shimadzu DTG-60H automatic derivatograph in an argon atmosphere in the temperature interval 30–500°C at a heating rate of 3 deg min^{-1} .

The X-ray photoelectron spectra were recorded with an EMS-3 automatic X-ray photoelectron spectrometer (Udmurt Federal Research Center, Ural Branch, Russian Academy of Sciences) using AlK_α radiation ($h\nu = 1486.6$ eV). The samples were rubbed in the moist surface of a pyrolytic graphite support and immediately placed into the working chamber of the spectrometer. The residual pressure in the working chamber of the spectrometer did not exceed 10^{-5} Pa. The energy scale was calibrated with respect to the C1s peak assuming $E_B(\text{C1s}) = 285$ eV. We recorded the core level $\text{Cu}2p$, $\text{Cu}3s$, $\text{P}2p$, $\text{Zn}3s$, $\text{O}1s$, and $\text{N}1s$ spectra and the valence band ($E_B = 0$ –30 eV) spectra. The samples were heated in situ (in the working chamber of the spectrometer) in the temperature interval 100–450°C using the built-in heating attachment.

Statistical processing of the experimental data, including determination of the measurement uncertainty, Shirley subtraction of the background from inelastically scattered electrons [11], and determination of the intensity of separate spectrum lines, was performed with Fityk 0.9.8 program.

RESULTS AND DISCUSSION

Thermal gravimetric and differential thermal analysis of all the complexes (Fig. 2) reveals a strong endothermic effect in a wide temperature interval 40–200°C with the heat absorption maximum at 64°C, corresponding to the loss of 11 water molecules. For the complex $\text{Na}_4[\text{Cu}_{1/4}\text{Zn}_{3/4}\text{N}(\text{CH}_2\text{PO}_3)_3] \cdot 13\text{H}_2\text{O}$ in the interval 280–340°C, the weight loss corresponding to $1/2\text{NH}_3$ without thermal effect is observed. The temperature dependence of the integral intensity of the $\text{N}1s$ X-ray photoelectron spectrum (Fig. 3) confirms the loss of approximately $1/2\text{N}$ (half of nitrilotris(methylenephosphonic) acid molecules) at approximately 300°C.

In the interval 390–440°C, there is an exothermic effect with the maximum at 420°C and the weight loss corresponding to a methanol molecule. The exothermic effect in the interval 440–490°C, manifested as a shoulder in the $Q(T)$ curve, corresponds to the loss of $1/2\text{NH}_3$ and is accompanied by a decrease in the integral intensity of the $\text{N}1s$ X-ray photoelectron spectrum almost to zero.

Thermal decomposition of the complex $\text{Na}_4[\text{Cu}_{1/2}\text{Zn}_{1/2}\text{N}(\text{CH}_2\text{PO}_3)_3] \cdot 13\text{H}_2\text{O}$ in the interval 250–

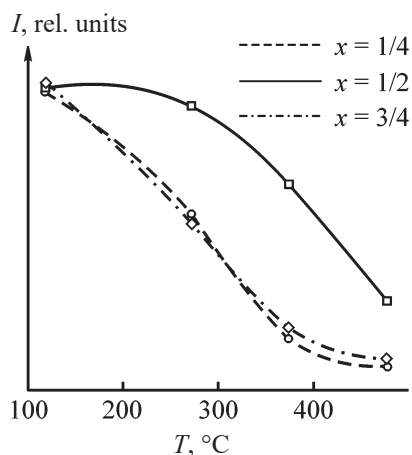


Fig. 3. Integral intensity of the N1s X-ray photoelectron spectrum of the complexes $\text{Na}_4[\text{Cu}_x\text{Zn}_{1-x}\text{N}(\text{CH}_2\text{PO}_3)_3] \cdot 13\text{H}_2\text{O}$ at $x = 1/4, 1/2,$ and $3/4$ as a function of temperature.

290°C is characterized by an exothermic effect with the maximum at 266°C without weight loss. The integral intensity of the N1s X-ray photoelectron spectrum does not noticeably decrease in this temperature interval. The exothermic effect in the interval 300–408°C with the maximum at 385°C corresponds to the loss of nitrogen in the form of NH_3 and agrees with a sharp decrease in the integral intensity of the N1s X-ray photoelectron spectrum in this temperature interval. The exothermic effect in the interval 408–420°C with the maximum at 413°C is accompanied by a slight increase in the sample weight. This may be due to the uptake of a small amount of water from air.

Thermal decomposition of the complex $\text{Na}_4[\text{Cu}_{3/4}\text{Zn}_{1/4}\text{N}(\text{CH}_2\text{PO}_3)_3] \cdot 13\text{H}_2\text{O}$ is accompanied by two pronounced exothermic effects with the maxima at 230 and 260°C and no weight loss. They correspond to the rearrangement of the internal molecular structure. In the interval 280–350°C, there is an exothermic effect with the maximum at 335°C and loss of $(\text{H}_2\text{O} + 1/2\text{NH}_3)$, and in the interval 350–375°C, an exothermic effect with the maximum at 365°C and loss of $1/2\text{NH}_3$. The integral intensity of the N1s X-ray photoelectron spectrum correspondingly decreases in these intervals. The exothermic effect in the interval 375–390°C with the maximum at 378°C and small (about $1/4\text{H}_2\text{O}$) weight gain is due to the water uptake from air.

Thus, the thermal stability of the compounds studied can be characterized both by the temperature at which the molecular structure starts to change and by the

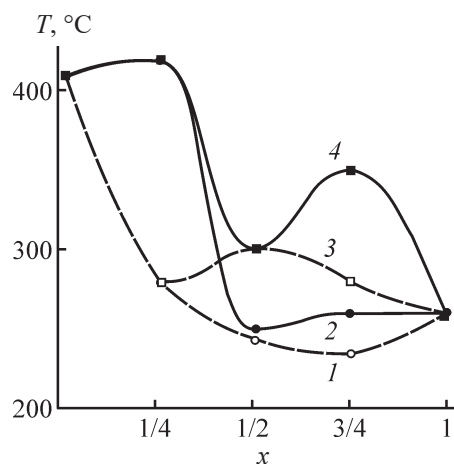


Fig. 4. Temperatures of the (1, 2) onset of changes in the molecular structure of the complexes $\text{Na}_4[\text{Cu}_x\text{Zn}_{1-x}\text{N}(\text{CH}_2\text{PO}_3)_3] \cdot 13\text{H}_2\text{O}$ and (3, 4) weight loss onset as functions of the Cu mole fraction x .

temperature at which the sample starts to lose weight through elimination of gaseous products (Fig. 4).

Analysis of the X-ray photoelectron spectra of the initial complexes $\text{Na}_4[\text{Cu}_x\text{Zn}_{1-x}\text{N}(\text{CH}_2\text{PO}_3)_3] \cdot 13\text{H}_2\text{O}$ at $x = 1/4, 1/2,$ and $3/4$ (Fig. 5) shows that all the phosphorus atoms are in the equivalent chemical state (are bound to the metal atom via oxygen atom of the PO_3 group); this follows from the presence of only a single peak in the P2p photoelectron spectrum with the maximum at the binding energy $E_B = 133.5\text{--}133.7$ eV. In the Zn3s photoelectron spectrum, there is also only one peak with $E_B = 139.7\text{--}139.8$ eV. The Cu2p photoelectron spectrum has a complex structure characteristic of transition metals with the incompletely filled 3d shell. It contains a typical $\text{Cu}2p_{3/2}\text{--Cu}2p_{1/2}$ spin-orbit doublet with the binding energies of the constituents $E_B = 932.5\text{--}933.0$ and $952.8\text{--}953.2$ eV, respectively. Each constituent of the Cu2p doublet has several strong satellites suggesting differences in the electronic structure of the coordination surrounding of the copper atom in the complexes with $x = 1/4, 1/2,$ and $3/4$. The intensity of the spectrum lines corresponding to the atoms of the complex-forming metals varies in proportion with the copper fraction x in the complexes.

Thermal decomposition leads to changes in the structure of the complexes $\text{Na}_4[\text{Cu}_x\text{Zn}_{1-x}\text{N}(\text{CH}_2\text{PO}_3)_3] \cdot 13\text{H}_2\text{O}$ (Fig. 5, curve 4). The P2p spectrum becomes noticeably broadened, which indicates that the nearest surrounding of the phosphorus atoms in the decomposition products is nonequivalent. The intensity maximum in the Zn3s

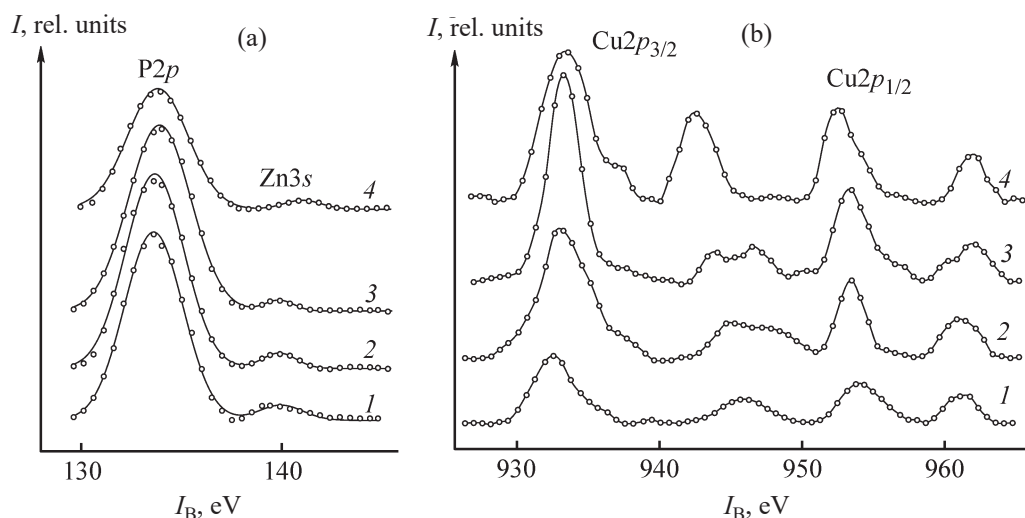


Fig. 5. Fragments of the X-ray photoelectron spectra [(a) P2p and Zn3s; (b) Cu2p] of the complexes $\text{Na}_4[\text{Cu}_x\text{Zn}_{1-x}\text{N}(\text{CH}_2\text{PO}_3)_3] \cdot 13\text{H}_2\text{O}$ at $x = (1) 1/4, (2) 1/2, (3) 1/4$ at 120°C and (4) of decomposition products of the complex $\text{Na}_4[\text{Cu}_{1/2}\text{Zn}_{1/2}\text{N}(\text{CH}_2\text{PO}_3)_3] \cdot 13\text{H}_2\text{O}$ at 475°C .

spectrum is shifted toward higher binding energies ($E_B = 140.7\text{--}139.8\text{ eV}$), which indicates that the electron density is shifted from the zinc atom toward oxygen atoms in its surrounding, i.e., that the Zn–O bond becomes more ionic. The constituents of the Cu2p spin-orbit doublet also become broadened, and the intensity of their satellites appreciably increases.

The observed differences in the decomposition onset temperatures and mechanisms of thermal decomposition of heterometallic complexes $\text{Na}_4[\text{Cu}_x\text{Zn}_{1-x}\text{N}(\text{CH}_2\text{PO}_3)_3] \cdot 13\text{H}_2\text{O}$ and monometallic $\text{Na}_4[\text{ZnN}(\text{CH}_2\text{PO}_3)_3] \cdot 13\text{H}_2\text{O}$ and $\text{Na}_4[\text{CuN}(\text{CH}_2\text{PO}_3)_3] \cdot 13\text{H}_2\text{O}$, shown most clearly in Fig. 4, can be rationalized with the following assumptions:

- the nitrilotris(methylenephosphonic) acid molecule coordinated by the Cu atom decomposes more readily (at a lower temperature) than that coordinated by the Zn atom;

- the inner coordination sphere of the metals in all the examined crystalline complexes contains two nitrilotris(methylenephosphonic) acid molecules, each of which is coordinated to either Cu or Zn atom.

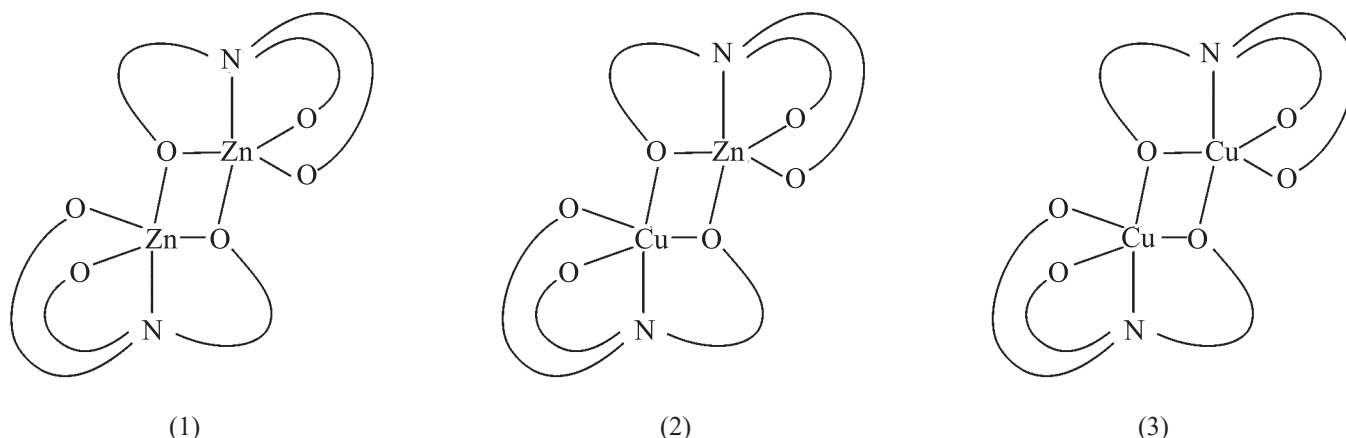
Thus, the inner coordination sphere of each structural unit in the crystalline complexes $\text{Na}_4[\text{Cu}_x\text{Zn}_{1-x}\text{N}(\text{CH}_2\text{PO}_3)_3] \cdot 13\text{H}_2\text{O}$ can be presented by one of the following structures (Scheme 1).

The crystal structure of the monometallic complexes $\text{Na}_4[\text{ZnN}(\text{CH}_2\text{PO}_3)_3] \cdot 13\text{H}_2\text{O}$ and $\text{Na}_4[\text{CuN}(\text{CH}_2\text{PO}_3)_3] \cdot 13\text{H}_2\text{O}$, studied previously [8], is built of clusters of only one type, (1) and (3), respectively. Therefore, the thermal decomposition mechanism is relatively simple, and the characteristic temperature points in Fig. 4 coincide.

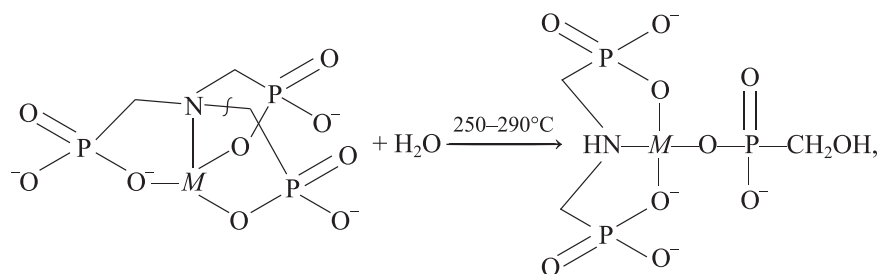
The replacement of $1/4$ of the zinc atoms in the structure of $\text{Na}_4[\text{ZnN}(\text{CH}_2\text{PO}_3)_3] \cdot 13\text{H}_2\text{O}$ leads to the structure described by the formula $\text{Na}_4[\text{Cu}_{1/4}\text{Zn}_{3/4}\text{N}(\text{CH}_2\text{PO}_3)_3] \cdot 13\text{H}_2\text{O}$. This formula can correspond both to a combination of $3/4$ structural unit (1) with $1/4$ structural unit (3) and to a combination of $1/2$ structural unit (1) with $1/2$ structural unit (2); more complex structures indiscernible by X-ray diffraction analysis are also possible. The fact that the thermal decomposition of $\text{Na}_4[\text{Cu}_{1/4}\text{Zn}_{3/4}\text{N}(\text{CH}_2\text{PO}_3)_3] \cdot 13\text{H}_2\text{O}$ in the interval $280\text{--}340^\circ\text{C}$ is accompanied by the loss of $1/2\text{NH}_3$ counts in favor of a combination of $1/2$ structural unit (1) with $1/2$ structural unit (2). Clusters (2) with the more strained structure are probably the constituents that decompose in the interval $280\text{--}340^\circ\text{C}$.

The bond dissociation energy determined by electron impact mass spectrometry, according to the published data, is 226 kJ mol^{-1} for the C–N bond in the triethylamine ($\text{N}(\text{CH}_3)_3$) molecule [12] and 477 kJ mol^{-1} for the C–P bond in the methylphosphine (H_2PCH_3) molecule [13]. Hence, in thermal decomposition of the

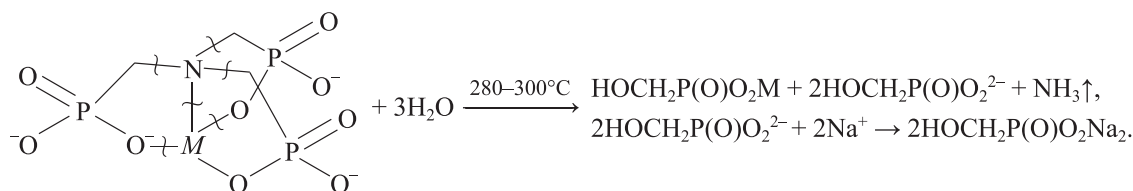
Scheme 1.



Scheme 2.



Scheme 3.



ligand molecule, the C–N bond should be expected to be cleaved first. This agrees with the fact that, when heated to 100°C for 9 days in the presence of excess Cu²⁺ ions, nitrilotris(methylenephosphonic) acid decomposed with the formation of iminobis(methylenephosphonic) acid zwitterion H₂N⁺(CH₂PO₃H₂)(CH₂PO₃H⁻), which was confirmed by the X-ray diffraction analysis of the copper complex [14, 15].

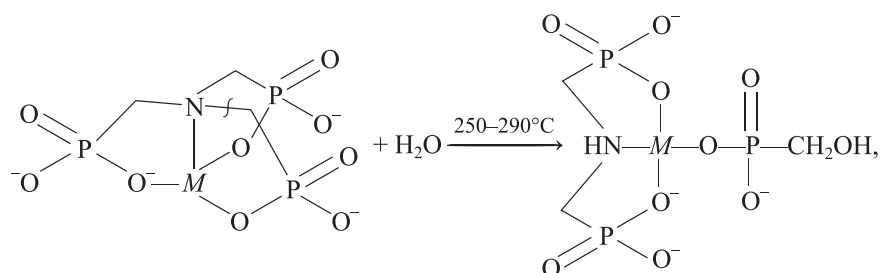
We believe that the C–N bonds in the nitrilotris(methylenephosphonic) acid molecule are cleaved by the hydrolytic mechanism Scheme 2.

The methanol elimination in the interval 390–440°C probably occurs in accordance with the scheme

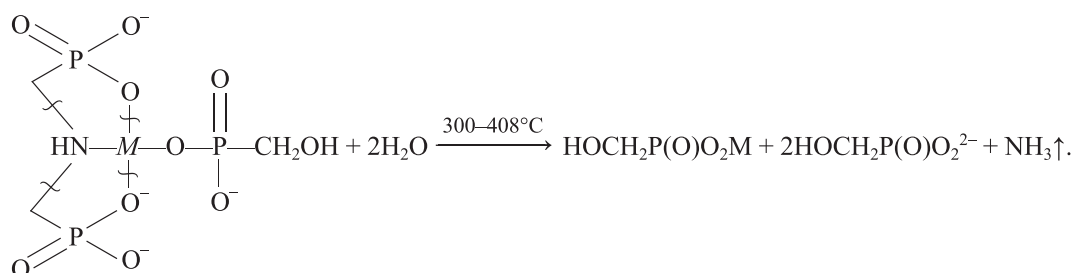


The exothermic effect in the interval 440–490°C corresponds to decomposition of clusters (1) in accordance with Scheme 3. The transformation of the complex Na₄[Cu_{1/2}Zn_{1/2}N(CH₂PO₃)₃]·13H₂O in the temperature interval 250–290°C without weight changes can be described, in our opinion, by the following scheme involving formation of a heteroligand complex

Scheme 4.



Scheme 5.



(Scheme 3), which agrees with the C–N bond cleavage and formation of iminobis(methylenephosphonic) acid according to [14, 15]. The nitrogen loss in the interval 300–408°C is probably due to thermal decomposition of the heteroligand complex (Scheme 4).

Two exothermic effects at 230 and 260°C, observed in the course of thermal decomposition of the complex $\text{Na}_4[\text{Cu}_{3/4}\text{Zn}_{1/4}\text{N}(\text{CH}_2\text{PO}_3)_3] \cdot 13\text{H}_2\text{O}$, are most probably due to transformations of clusters (3) and (2), respectively, in accordance with Scheme 4. The nitrogen elimination in the intervals 280–350 and 350–375°C from clusters (3) and (2) is described by Scheme 5.

The thermal stability of all the complexes studied (Fig. 4) is the lower, the larger is the difference between the interatomic distances (Table 1) in the base of the coordination polyhedron (trigonal bipyramid) of the metal atom, i.e., between the longest distance $d(\text{M}^1-\text{O}^1)$ and the shortest distances $d(\text{M}^1-\text{O}^{9A})$ and $d(\text{M}^1-\text{O}^5)$. This fact suggests that the main cause of cleavage of the ligand molecule is the Baeyer strain in chelate rings.

Differences in the interatomic distances in the surrounding of the copper atom (Table 1) agree also with differences in the satellite structure observed in the $\text{Cu}2p$ electron spectra of the corresponding complexes (Fig. 5b) [16, 17]. However, the mechanism of the formation of the corresponding satellites in the spectra is

not fully understood [18], which complicates structural-chemical interpretation of the spectrum features and requires further studies. Thermal decomposition leads to changes in the satellite structure, which becomes close to that in the spectrum of $\text{Cu}_3(\text{PO}_4)_2$ [16, 17]. As we showed previously [6], the monometallic complex $\text{Na}_4[\text{ZnN}(\text{CH}_2\text{PO}_3)_3] \cdot 13\text{H}_2\text{O}$ decomposes on heating to zinc peroxides and phosphates, and the complex $\text{Na}_4[\text{CuN}(\text{CH}_2\text{PO}_3)_3] \cdot 13\text{H}_2\text{O}$, to copper hydrophosphate and sodium pyrophosphate. The same compounds are probably formed in different ratios upon decomposition of heterometallic complexes $\text{Na}_4[\text{Cu}_x\text{Zn}_{1-x}\text{N}(\text{CH}_2\text{PO}_3)_3] \cdot 13\text{H}_2\text{O}$.

CONCLUSION

Combination of thermal gravimetric and differential thermal analysis and X-ray photoelectron spectroscopy with the thermal action in situ furnishes new information on the thermochemical behavior and mechanism of thermal decomposition of heterometallic complexes $\text{Na}_4[\text{Cu}_x\text{Zn}_{1-x}\text{N}(\text{CH}_2\text{PO}_3)_3] \cdot 13\text{H}_2\text{O}$ ($0 < x < 1$) compared to the results of single crystal X-ray diffraction analysis.

In particular, water of crystallization is eliminated from all the complexes studied in a wide temperature interval, 40–200°C. The complexes $\text{Na}_4[\text{Cu}_{1/4}\text{Zn}_{3/4}\text{N}(\text{CH}_2\text{PO}_3)_3] \cdot 13\text{H}_2\text{O}$ and

$\text{Na}_4[\text{Cu}_{3/4}\text{Zn}_{1/4}\text{N}(\text{CH}_2\text{PO}_3)_3] \cdot 13\text{H}_2\text{O}$ decompose at approximately 280°C in two steps in accordance with differences between the complex anions containing monometallic and heterometallic M–O–M–O rings. The complex $\text{Na}_4[\text{Cu}_{1/2}\text{Zn}_{1/2}\text{N}(\text{CH}_2\text{PO}_3)_3] \cdot 13\text{H}_2\text{O}$ starts to decompose in the interval 250–290°C with an exothermic transformation without elimination of volatile products; the loss of nitrogen in the form of ammonia occurs at approximately 300°C. The mechanism of the thermal decomposition of $\text{Na}_4[\text{Cu}_{3/4}\text{Zn}_{1/4}\text{N}(\text{CH}_2\text{PO}_3)_3] \cdot 13\text{H}_2\text{O}$ is the most complex. It involves two exothermic transformations and two steps of the decomposition of intermediates with the loss of nitrogen in the form of ammonia. The complex $\text{Na}_4[\text{Cu}_{1/4}\text{Zn}_{3/4}\text{N}(\text{CH}_2\text{PO}_3)_3] \cdot 13\text{H}_2\text{O}$ is characterized by the highest decomposition onset temperature (280°C), and the complex $\text{Na}_4[\text{Cu}_{1/2}\text{Zn}_{1/2}\text{N}(\text{CH}_2\text{PO}_3)_3] \cdot 13\text{H}_2\text{O}$, by the highest weight loss onset temperature (300°C).

ACKNOWLEDGMENTS

The study was performed using the equipment of the Surface and New Materials Center for Shared Use, Udmurt Federal Research Center, Ural Branch, Russian Academy of Sciences.

FUNDING

The study was performed in accordance with research plan no. 121030100002-0 of the Ministry of Science and Higher Education of the Russian Federation.

CONFLICT OF INTEREST

The authors declare that they have no conflict of interest.

AUTHOR CONTRIBUTION

F.F. Chausov: development of the program of the study, processing and comparison of the results, and formulation of the main conclusions; I.S. Kazantseva: synthesis and purification of samples of heterometallic complexes, preparation of single crystals, and elemental analysis of the samples; N.V. Lomova, A.V. Kholzakov, and I.N. Shabanova: X-ray photoelectron spectroscopy of the heterometallic complexes and processing and interpretation of the experimental data obtained; N.E. Suksin: TGA/DTA study of the heterometallic complexes.

REFERENCES

1. Demadis, K.D., Katarachia, S.D., and Koutmos, M., *Inorg. Chem. Commun.*, 2005, vol. 8, pp. 254–258.

- <https://doi.org/10.1016/j.inoche.2004.12.019>
2. Somov, N.V. and Chausov, F.F., *Crystallogr. Rep.*, 2014, vol. 59, no. 1, pp. 66–70.
<https://doi.org/10.1134/S1063774513050118>
3. Chausov, F.F., Kazantseva, I.S., Reshetnikov, S.M., Lomova, N.V., Maratkanova, A.N., and Somov, N.V., *Chem. Select*, 2020, vol. 5, no. 43, pp. 13711–13719.
<https://doi.org/10.1002/slct.202003255>
4. Somov, N.V. and Chausov, F.F., *Crystallogr. Rep.*, 2015, vol. 60, no. 2, pp. 210–216.
<https://doi.org/10.1134/S1063774515010228>
5. Somov, N.V., Chausov, F.F., Kazantseva, I.S., Maratkanova, A.N., and Nikitina, M.N., *Polyhedron*, 2021, vol. 195, ID 114964.
<https://doi.org/10.1016/j.poly.2020.114964>
6. Chausov, F.F., Zakirova, R.M., Somov, N.V., Petrov, V.G., Aleksandrov, V.A., Shumilova, M.A., Naimushina, E.A., and Shabanova, I.N., *Russ. J. Appl. Chem.*, 2014, vol. 87, no. 8, pp. 1031–1037.
<https://doi.org/10.1134/S1070427214080047>
7. Kazantseva, I.S., Chausov, F.F., Fedotova, I.V., and Sapozhnikov, G.V., *Chem. Phys. Mesosc.*, 2019, vol. 21, no. 4, pp. 589–597.
<https://doi.org/10.15350/17270529.2019.4.62>
8. Gaines, P.C. and Woodruff, R., *J. Chem. Educ.*, 1949, vol. 26, no. 3, pp. 166–167.
<https://doi.org/10.1021/ED026P166>
9. Chou, Y.-H., Yu, J.-H., Liang, Y.-M., Wang, P.-J., and Chen, S.-S., *Chemosphere*, 2015, vol. 141, pp. 183–188.
<https://doi.org/10.1016/j.chemosphere.2015.07.016>
10. <http://www.ccdc.cam.ac.uk/conts/retrieving.html>.
CCDC 919565 ($\text{Na}_4[\text{ZnN}(\text{CH}_2\text{PO}_3)_3] \cdot 13\text{H}_2\text{O}$), 2024334 ($\text{Na}_4[\text{Cu}_{0.253}\text{Zn}_{0.747}\text{N}(\text{CH}_2\text{PO}_3)_3] \cdot 13\text{H}_2\text{O}$), 2024337 ($\text{Na}_4[\text{Cu}_{0.515}\text{Zn}_{0.485}\text{N}(\text{CH}_2\text{PO}_3)_3] \cdot 13\text{H}_2\text{O}$), 2024389 ($\text{Na}_4[\text{Cu}_{0.725}\text{Zn}_{0.275}\text{Cu}_x\text{Zn}_{1-x}\text{N}(\text{CH}_2\text{PO}_3)_3] \cdot 13\text{H}_2\text{O}$), and 1908017 ($\text{Na}_4[\text{CuN}(\text{CH}_2\text{PO}_3)_3] \cdot 13\text{H}_2\text{O}$).
11. Shirley, D.A., *Phys. Rev. B*, 1972, vol. 5, pp. 4709–4714.
<https://doi.org/10.1103/physrevb.5.4709>
12. Collin, J., *Bull. Soc. Chim. Belg.*, 1953, vol. 62, nos. 7–8, pp. 411–427.
<https://doi.org/10.1002/bscb.19530620707>
13. Wada, Y. and Kiser, R.W., *J. Phys. Chem.*, 1964, vol. 68, no. 8, pp. 2290–2295.
<https://doi.org/10.1021/j100790a044>

14. Cabeza, A., Bruque, S., Guagliardi, A., and Aranda, M.A.G., *J. Solid State Chem.*, 2001, vol. 160, pp. 278–286.
<https://doi.org/10.1006/jssc.2001.9246>
15. Cabeza, A., Ouyang, X., Sharma, C.V.K., Aranda, M.A.G., Bruque, S., and Clearfield, A., *Inorg. Chem.*, 2002, vol. 41, no. 9, pp. 2325–2333.
<https://doi.org/10.1021/ic0110373>
16. Biesinger, M.C., *Surf. Interface Anal.*, 2017, vol. 49, pp. 1325–1334.
<https://doi.org/10.1002/sia.6239>
17. Biesinger, M.C., Lau, L.W.M., Gerson, A.R., and Smart, R.St.C., *Appl. Surf. Sci.*, 2010, vol. 257, no. 3, pp. 887–898.
<https://doi.org/10.1016/j.apsusc.2010.07.086>
18. Brundle, C.R. and Crist, B.V., *J. Vacuum Sci. Technol. A*, 2020, vol. 38, no. 4, ID 041001.
<https://doi.org/10.1116/1.5143897>